Nature of the Deconfining Phase Transition in SU(3) Lattice Gauge Theory

Frank R. Brown, Norman H. Christ, Yuefan Deng, Mingshen Gao, and Thomas J. Woch
Department of Physics, Columbia University, New York, New York 10027
(Received 3 August 1988)

Monte Carlo calculations on lattices with large spatial volume show that the SU(3) deconfining phase transition is more weakly first order than previously thought. We have studied the transition for $N_T=4$ and 6 on lattices of spatial volumes 16^3, 20^3, and 24^3. The $24^3\times4$ calculations show a sharp first-order phase transition, yielding a latent heat $\Delta\mathcal{E}/T^4$ of 2.54 ± 0.12. The $24^3\times6$ calculations suffer greater finite-volume smearing, but suggest that $\Delta\mathcal{E}/T^4=2.48\pm0.24$. Correlation lengths increase significantly near the transition, and the energy plus pressure of the ordered phase depends strongly on β.

PACS numbers: 11.15.Ha, 05.50.+q, 12.38.Gc

Numerous Monte Carlo studies of pure SU(3) lattice gauge theory have focused on the deconfining phase transition that occurs at finite temperature. This transition is expected to be first order,[1] and significant numerical effort has been invested in the determination of the associated latent heat.[2-6] The rather small spatial volumes employed smear out the phase transition, introducing uncertainties into estimates of the latent heat. We have undertaken a series of deconfinement calculations with relatively large spatial volumes that have led us to revise somewhat our understanding of the nature of the deconfining phase transition.

Our large-volume calculations employ both a large lattice and a large lattice spacing; simulations on $24^3\times N_T$ lattices are carried out on the 64-node Columbia University Parallel Supercomputer, a 1-gigaflop, 128-megabyte machine,[7] and the small temporal extents $N_T=4$ and 6 yield large lattice spacings. (These lattice spacings are large enough to introduce significant deviations from continuum behavior.[8,9])

Our calculations use the standard Wilson action, and are performed with a modified[10,11] Cabibbo-Marinari update. The data[6] for the spatial volumes 16^3 and 20^3 were obtained with our 16-node computer,[12] and the 24^3 results are from our 64-node machine. On both machines we compute for each sweep the spatial average of the real and imaginary parts of the Polyakov loop observable $P(\mathbf{r})$:

$$P(\mathbf{r})=\tfrac{1}{3}\,\mathrm{tr}\left(\prod_l U_l\right).$$

Here the product is taken over all temporal link matrices U_l with spatial coordinates $\mathbf{r}$. In addition, 1×1 Wilson loops with space-space and space-time orientations are separately averaged over the lattice for each Monte Carlo sweep.

With use of standard formulas[13] the sum and difference of these plaquette expectation values determine the quantities $\mathcal{E}-3\mathcal{P}$ and $\mathcal{E}+\mathcal{P}$, respectively:

$$\mathcal{E}-3\mathcal{P}=\frac{16}{N_S^3N_T}[0.01742+O(g^2)]\left\{\sum_{n,i}\mathrm{tr}U(n)_{0,i}+\sum_{n,i<j}\mathrm{tr}U(n)_{i,j}\right\},$$

$$\mathcal{E}+\mathcal{P}=\frac{4\beta}{4N_S^3N_T}[1-0.16678g^2+O(g^4)]\left\{\sum_{n,i}\mathrm{tr}U(n)_{0,i}-\sum_{n,i<j}\mathrm{tr}U(n)_{i,j}\right\}.$$

The matrix $U(n)_{\mu,\nu}$ is the elementary plaquette lying in the μ-ν plane at the location n, while the sums run over all space-time locations n and spatial directions i and j. $\mathcal{E}$ and $\mathcal{P}$ are the energy density and pressure of the system, respectively. Their sum, the entropy of the system,[14] is finite in the continuum limit, but shows large statistical fluctuations. Although the other combination $\mathcal{E}-3\mathcal{P}$ contains a divergent vacuum contribution it is no harder to determine absolutely.[5] Because the pressure is continuous across the transition the discontinuity in either of these quantities yields $\Delta\mathcal{E}$, the latent heat.

On the 24^3 lattices we also calculate the Polyakov loop correlations for each separation $\mathbf{r}$:

$$\mathcal{C}(\mathbf{r})=\frac{1}{N_S^3}\sum_{\mathbf{r}'}\langle P(\mathbf{r}+\mathbf{r}')P(\mathbf{r}')^*\rangle.$$

Here the angular brackets represent a Monte Carlo average and the variable $\mathbf{r}'$ varies over the entire 24^3 spatial volume. We determine correlation lengths from least-squares fits of $\mathcal{C}(\mathbf{r})$ to two simple theoretical forms. For confined values of β we use a sum of eight Boltzmann factors corresponding to a string potential between the quark at $\mathbf{r}+\mathbf{r}'$ and the quark at $\mathbf{r}'$ (or one of its seven reflections in our periodic boundaries):

$$\mathcal{C}(\mathbf{r})=\sum_{i=1,8}Z\exp\left(-N_T\sigma|\mathbf{r}-\mathbf{r}_i|-\frac{c}{|\mathbf{r}-\mathbf{r}_i|}\right).$$

The sum over r_i runs over the eight corners of a 24^3 cube. Stable fits for Z, σ, and c are obtained with a minimum fitting radius $r_{\min}$ that can vary between 2.0

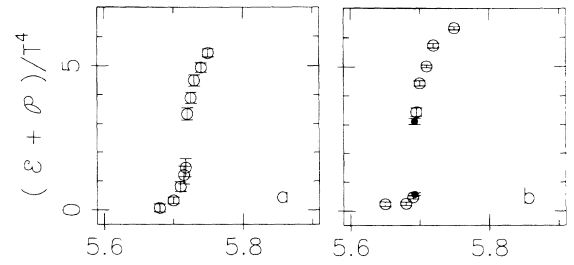

FIG. 1. The quantity $\mathcal{E}+\mathcal{P}$ computed on (a) $16^3\times4$ and (b) $24^3\times4$ lattices as a function of β. The 16^3 points each represent typically 15000 sweeps except for the three points with β between 5.71 and 5.7175 which contain $\sim$50000 heat-bath sweeps each. The 24^3 points are all averages over 20000 sweeps, except for the two solid points which were obtained by our dividing a single 60000-sweep $\beta=5.6925$ run into confined and deconfined sections.

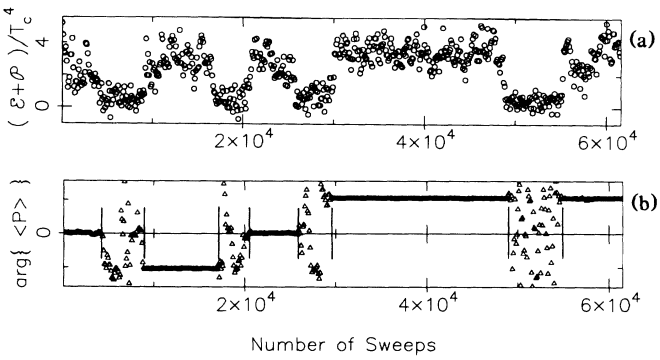

FIG. 2. The evolution with Monte Carlo time of (a) $\mathcal{E}+\mathcal{P}$ and (b) the argument of the Polyakov loop on a $24^3\times4$ lattice for $\beta=5.6925$. Each point represents an average over a block of 100 sweeps. The vertical lines mark the tunneling events (identified by eye) used to separate the run into confined and deconfined sections.

and 6.0. For deconfined values of β we fit to a single Boltzmann factor describing a screened Yukawa potential between one of the quarks and the eight images of the other:

$$\mathcal{C}(\mathbf{r})=P\exp\sum_{i=1,8}\left(-G\frac{\exp(-\mu|\mathbf{r}-\mathbf{r}_i|)}{|\mathbf{r}-\mathbf{r}_i|}\right).$$

We obtain stable values of the constants P, G, and μ for a minimum fitting radius which varies between 4.0 and 8.0. The errors in both of these fits are determined directly from the fluctuations seen in the results if the data are divided into four blocks and each block is separately fitted.

Unfortunately the important task of our comparing the 16^3 and 24^3 volumes is made difficult by the systematic differences between the entirely different programs used on our two machines. The 64-node program (24^3 volumes) is believed to achieve an accuracy close to the 32-bit precision of the machine. However, the 16-node program (16^3 and 20^3 volumes) gives observables off by a few tenths of a percent, ten times worse than the inherent 22-bit precision of the 16-node hardware. Although we have not yet located the source of this error, we have observed that this discrepancy can be compensated for by associating with the 16-node calculations an effective value of β approximately 0.02 smaller than that actually used. We will assume that no other correction is required to compare the results of the two machines. (To the best of our knowledge, this is consistent with all of our data.)

Our principal results concern the behavior of $\mathcal{E}+\mathcal{P}$ in the transition region. Figure 1 shows $\mathcal{E}+\mathcal{P}$ as a function of β for $N_T=4$ and spatial lattice sizes of both 16^3 and 24^3. Note the clear discontinuity in $\mathcal{E}+\mathcal{P}$ seen on the 24^3 lattice and the rapid (but continuous) drop in $\mathcal{E}+\mathcal{P}$ as the transition is approached from above. We argue that this correctly reflects the behavior of the infinite-volume limit; the agreement (after accounting for the effective shift in β discussed above) between the 16^3 and 24^3 curves precludes the possibility that finite-volume smearing has rounded a large discontinuity into a rapid continuous drop plus a smaller discontinuity. (Conversely, the rise in $\mathcal{E}+\mathcal{P}$ shown by the 16^3 calculation as the transition is approached from below is seen to be due to finite-volume smearing because it is absent in the 24^3 calculation.) The latent heat can be read directly off Fig. 1(b); we obtain $\Delta\mathcal{E}/T^4=\Delta(\mathcal{E}+\mathcal{P})/T^4=2.54\pm0.12$.

The two solid points in Fig. 1(b) were obtained from a single run divided by hand into separate phases. In Fig. 2, this Monte Carlo evolution is displayed, together with the tunneling events as identified by eye. The coexistence of both phases at a single value of β also permits us to obtain the latent heat from the discontinuity in $\mathcal{E}-3\mathcal{P}$, an approach that is otherwise hindered by the strong dependence of $\mathcal{E}-3\mathcal{P}$ on β; we obtain $\Delta\mathcal{E}/T^4=\Delta(\mathcal{E}-3\mathcal{P})/T^4=3.78\pm0.20$. This difference between this estimate of the latent heat and the value of $\Delta(\mathcal{E}+\mathcal{P})$ given above reflects the errors introduced by finite-lattice spacing; they should agree in the continuum limit. We prefer to quote values of $\Delta(\mathcal{E}+\mathcal{P})$ as the latent heat not because we believe it has smaller lattice spacing errors, but rather because $\mathcal{E}+\mathcal{P}$ depends much more weakly than $\mathcal{E}-3\mathcal{P}$ on β, making its discontinuity easier to resolve.

Figure 3 shows similar $\mathcal{E}+\mathcal{P}$ data for $N_T=6$. The presumed first-order nature of the transition is not as clearly resolved as it was on the $24^3\times4$ lattice. We suggest that at $N_T=6$ a 24^3 spatial lattice is not large enough to obtain fully unambiguous results, much as in Fig. 1 the structure seen in the $24^3\times4$ calculation is significantly degraded on the $16^3\times4$ lattice.

The curve in Fig. 3(b) indicates the assumptions about the "true" behavior of $\mathcal{E}+\mathcal{P}$ that underlie our determination of the latent heat, $\Delta\mathcal{E}/T^4=\Delta(\mathcal{E}+\mathcal{P})/T^4$

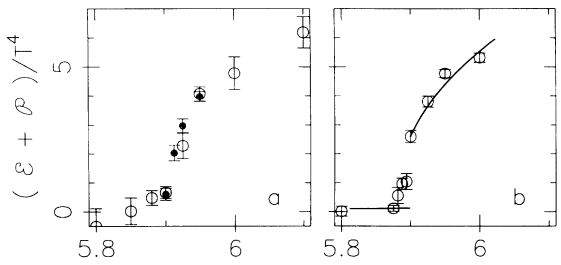

FIG. 3. The quantity $\mathcal{E}+\mathcal{P}$ computed on (a) $16^3\times6$ (open circles) and $20^3\times6$ (filled circles) and (b) $24^3\times6$ lattices as functions of β. The 16^3 and 20^3 points each represent between 10000 and 50000 heat-bath sweeps. The 24^3 points are derived from about 20000 sweeps each except for the three β values between 5.8875 and 5.90 which each contain approximately 100000 sweeps.

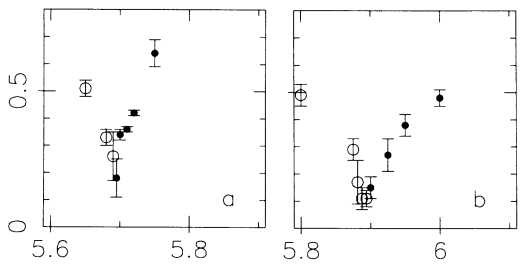

FIG. 4. Correlation lengths shown as a function of β on (a) $24^3\times4$ and (b) $24^3\times6$ lattices. The open circles correspond to confined values of β and the quantity plotted is the product of the string tension σ and N_T. The filled circles represent deconfined values of β and show the value of the Debye screening mass μ.

$=2.48\pm0.24$, as based on our experience with $N_T=4$. The rise in $\mathcal{E}+\mathcal{P}$ as the transition is approached from below is attributed to mixing of the phases (which is observed in the evolutions), and therefore discarded. On the other hand, the sharp drop in $\mathcal{E}+\mathcal{P}$ as the transition is approached from above is interpreted as the infinite-volume behavior of the ordered phase, and therefore retained. We report as the latent heat the difference of the end points of the two curves. The strong β dependence of $\mathcal{E}+\mathcal{P}$ in the ordered phase together with our use of a purely deconfined point as the ordered-phase end point is expected to yield a slight overestimate of the latent heat, an unknown systematic error introduced by finite-volume effects. (Using these assumptions to extract a latent heat from the $16^3\times4$ data yields results consistent with $24^3\times4$.)

A further indication of the complexity of the transition region comes from the behavior of the correlation lengths[15] shown in Fig. 4. (A typical fit is shown in Fig. 5.) On both sides of the transition the correlation length is seen to increase by a factor of 2 to 3 as the critical coupling β_c is approached. Although the falling string tension seen as $\beta\rightarrow\beta_c^-$ for $N_T=6$ may be interpreted as a finite-volume effect caused by the mixing of the two phases seen in the Monte Carlo time evolutions, such mixing is not seen for the points plotted for $N_T=4$ or the deconfined points for $N_T=6$. Note that the largest correlation length seen in these regions (7 ± 2 for $\beta=5.90$ and $N_T=6$) is still small compared to the largest diagonal separation (21.78) that is accessible to our analysis.

Thus the deconfining phase transition is seen to be weakly first order, with a rather small discontinuity in $\mathcal{E}+\mathcal{P}$ embedded in a rapid but continuous decrease in $\mathcal{E}+\mathcal{P}$ as the transition is approached from above, and with correlation lengths that increase significantly near the transition. Although this behavior might seem surprising, it is anticipated by that of the three-state Potts model in three dimensions.[16] The Potts model also displays a small latent heat embedded in a sharp crossover region, and in fact is interpreted as having near-critical behavior governed by a second-order fixed point in the superheated branch of the ordered phase. The similar structure seen in the deconfining phase transition makes it especially susceptible to finite-volume smearing, and therefore relatively large volumes are necessary to obtain accurate results.

We believe that two important conclusions can be drawn from the results presented here. First, the values of the latent heat [as obtained from $\Delta(\mathcal{E}+\mathcal{P})$], $\Delta\mathcal{E}/T^4=2.54\pm0.12$ and $\Delta\mathcal{E}/T^4=2.48\pm0.24$ for $N_T=4$ and 6, respectively, are 60% and 25% smaller than the earlier values.[2,3,6] Second, a comparison of the $16^3\times4$ and $24^3\times6$ curves, Figs. 1(a) and 3(b), shows that the rapid rise in $\mathcal{E}+\mathcal{P}$ following the transition for $N_T=4$ has broadened considerably for $N_T=6$ with a slope diminished by almost a factor of 3. This softening

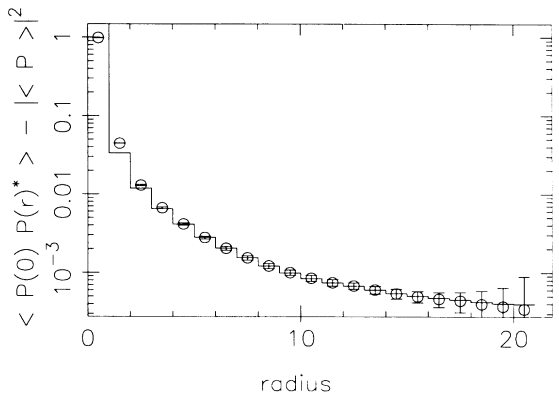

FIG. 5. The binned Polyakov-loop correlation function as a function of radius $|\mathbf{r}|$ for $\beta=5.90$ on a $24^3\times6$ lattice. The histogram shows the fit to a screened Yukawa potential from which the $\beta=5.90$ point in Fig. 4 was obtained.

of the structure in the transition region as N_T is increased may well continue as the continuum limit is approached. Altogether our calculations suggest a more nearly continuous transition than previously thought. If this behavior persists when the effects of dynamical quarks are included then the experimental effects of this phase transition will be more difficult to detect.

We thank Shigemi Ohta and Laurence Yaffe for numerous helpful discussions and Paul Hsieh for assistance with the 64-node program and much of the system software used during data collection. This work was supported in part by the U.S. Department of Energy.

[1]L. G. Yaffe and B. Svetitsky, Phys. Rev. D **26**, 963 (1982); B. Svetitsky, Phys. Rep. **132**, 1 (1986).

[2]J. Kogut *et al.*, Phys. Rev. Lett. **51**, 869 (1983).

[3]T. Çelik, J. Engels, and H. Satz, Phys. Lett. **129B**, 323 (1983).

[4]F. Karsch and R. Petronzio, Phys. Lett. **139B**, 403 (1984).

[5]S. Gottlieb *et al.*, Phys. Lett. B **189**, 181 (1987).

[6]N. H. Christ and H.-Q. Ding, Phys. Rev. Lett. **60**, 1367 (1988).

[7]M. Gao, in *Lattice Gauge Theory Using Parallel Processors,* edited by X. Y. Li, Z. M. Qiu, and H. C. Ren (Gordon and Breach, New York, 1987), p. 369.

[8]A. D. Kennedy *et al.*, Phys. Rev. Lett. **54**, 87 (1985).

[9]N. H. Christ and A. E. Terrano, Phys. Rev. Lett. **56**, 111 (1986).

[10]H.-Q. Ding, J. Comput. Phys. **67**, 28 (1986).

[11]Y. Deng, in Ref. 7, p. 419.

[12]N. H. Christ and A. E. Terrano, IEEE Trans. Comput. **33**, 344 (1984), and Byte **11**, No. 4, 145 (1986).

[13]J. Engles *et al.*, Nucl. Phys. **B205 [FS5]**, 545 (1982); F. Karsch, Nucl. Phys. **B205 [FS5]**, 285 (1982); B. Svetitsky and F. Fucito, Phys. Lett. **131B**, 165 (1983).

[14]S. Ohta, private communication.

[15]For earlier results on SU(3) screening lengths and finite-temperature string tension see M. Fukugita, T. Kaneko, and A. Ukawa, Phys. Lett. **154B**, 185 (1985), and T. A. DeGrand and C. E. DeTar, Phys. Rev. D **34**, 2469 (1986). The increasing screening length as $\beta \rightarrow \beta_c^+$ was observed by Yaffe and Svetitsky, Ref. 1, while the decreasing string tension as $\beta \rightarrow \beta_c^-$ was seen by Svetitsky, Ref. 1.

[16]H. W. J. Blöte and R. H. Swendsen, Phys. Rev. Lett. **43**, 799 (1979); H. J. Herrmann, Z. Phys. B **35**, 171 (1979); S. J. Knak Jensen and O. G. Mouritsen, Phys. Rev. Lett. **43**, 1736 (1979).